Journal of Organometallic Chemistry 808 (2016) 122–127

Contents lists available at ScienceDirect

Journal of Organometallic Chemistry

journal homepage: www.elsevier.com/locate/jorganchem

Communication

Iridium complexes inhibit tumor necrosis factor-α by utilizing light and mixed ligands

Elodie Sauvageot [a, b], Pierre Lafite [c, d], Eric Duverger [c, d, e], Ronan Marion [a, b], Matthieu Hamel [f], Sylvain Gaillard [a, b, **], Jean-Luc Renaud [a, b, ***], Richard Daniellou [c, d, *]

[a] Normandie University, University of Caen Normandie, Laboratoire de Chimie Moléculaire et Thioorganique, 14050 Caen, France
[b] CNRS, UMR 6507, 14050 Caen, France
[c] Univ. Orléans, CNRS, Institut de Chimie Organique et Analytique, 45067 Orléans, France
[d] CNRS, UMR 7311, 45067 Orléans, France
[e] Glycodiag, rue de Chartres, 45067 Orléans, France
[f] CEA, LIST, Laboratoire Capteurs et Architectures Electroniques, 91191 Gif-sur-Yvette Cedex, France

ARTICLE INFO

Article history:
Received 15 November 2015
Received in revised form
29 January 2016
Accepted 1 February 2016
Available online 18 February 2016

Keywords:
Iridium complexes
Inhibition
TNF-alpha
Light

ABSTRACT

We report herein a large study of the inhibition of tumor necrosis factor-α with 51 iridium(III) complexes, thus highlighting the influence of the nature of the ligands around the metal, their synergic effect and the role of the light.

1. Introduction

Since the discovery of the well-known cis-platin and its analogues, organometallic complexes have been widely used as anticancer drugs [1] and their biological studies are growing exponentially. This intense interest has been summarized in many reviews which nicely depict the state of the art of these researches in many diseases [2]. The principle advantage of transition metal complexes is their highly versatility for drug design. Besides variations in the metal and its oxidation state, metal ions have a range of geometries and coordination numbers that allow the fine-tuning for biological activities.

The tumor necrosis factor (TNF) superfamily plays highly diversified roles in the body but all members, without exception, exhibit pro-inflammatory activity, in part through activation of the transcription factor NF-κB [3]. Amongst them, the fascinating and heavily studied TNF-α demonstrated to play roles in inflammation, cellular proliferation, apoptosis and morphogenesis. In addition, its expression also proved to be linked with a wide variety of diseases, including cancer, diabetes, obesity, cardiovascular, neurologic, pulmonary, and autoimmune disorders. Thanks to that, TNF-α has become a tremendous active target for drug development in the last years. Novel therapies including anti-TNF antibodies such as Enbrel®, Humira®, Remicade® or Cimzia®, have significantly improved disease outcomes in patients suffering from a range of important inflammatory conditions including rheumatoid arthritis, psoriasis and Crohn's disease for examples. However and despite their success in the clinic, such antibodies suffer from important drawbacks, including poor tissue penetration, high manufacturing costs and frequent secondary effects like increase of cancer. As a consequence, there is an urgent need for alternatives. Following the pioneering work of He et al. with the compound SPD304 (Fig. 1) [4], small molecule modulation of this specific protein-protein interaction, *i.e.* able to transform an active TNF-α trimer into an inactive

* Corresponding author. Univ. Orléans, CNRS, Institut de Chimie Organique et Analytique, 45067 Orléans, France.
** Corresponding author. Normandie University, University of Caen Normandie, Laboratoire de Chimie Moléculaire et Thioorganique, 14050 Caen, France.
*** Corresponding author. Normandie University, University of Caen Normandie, Laboratoire de Chimie Moléculaire et Thioorganique, 14050 Caen, France.
E-mail addresses: sylvain.gaillard@ensicaen.fr (S. Gaillard), jean-luc.renaud@ensicaen.fr (J.-L. Renaud), richard.daniellou@univ-orleans.fr (R. Daniellou).

http://dx.doi.org/10.1016/j.jorganchem.2016.02.001
0022-328X/

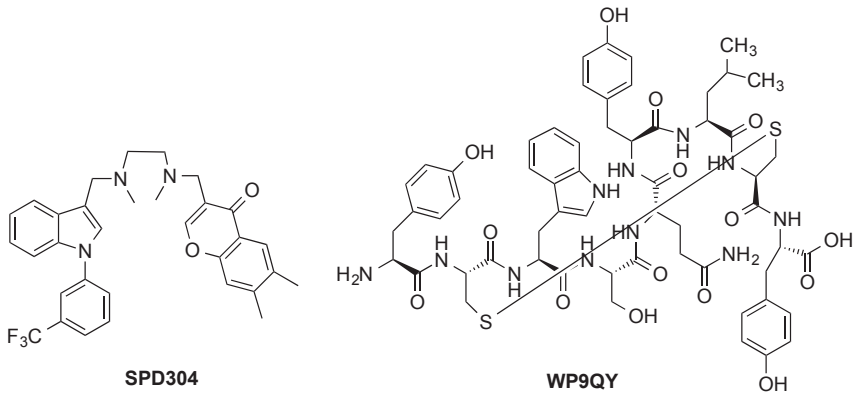

Fig. 1. Chemical structures of SPD304 and WP9QY.

dimer, has also been recognized as a promising approach in drug discovery [5]. For example, the antagonist cyclic peptide WP9QY (Fig. 1) demonstrated its efficiency in preventing both inflammatory bone destruction and systemic bone loss in rheumatoid arthritis [6]. Structured-based screening of chemical library of natural products has also led to the discovery of two potent small inhibitors, namely quinuclidine and indoloquinolizidine [7]. Moreover the screening of the SPECS database allowed the identification of original scaffolds with promising biological properties [8]. Besides, group 9 organometallic compounds have recently received an increased attention for their therapeutic and bioanalytical applications, mainly due to their ease of preparation, their stability in water and air, and their high solubility [9]. Amongst them, the team of Leung recently reported that the racemic (or even each enantiomer) iridium(III) complex, [Ir(ppy)$_2$(biq)][PF$_6$], was able to prevent the active trimer association through its interaction with β-strands of the TNF-α dimer, and exhibited an IC$_{50}$ of 22 μM in ELISA experiments against the TNF-α/TNFR1 interaction, comparable with SPD304 [10].

Since several years, we have developed a research program devoted to the synthesis [11], the coordination [12], and the reactivity of metal complexes coordinated to dipyridylamine derivatives. We have recently reported the synthesis and the characterization of a series of neutral and cationic cyclometalated iridium(III) complexes bearing both C^N ligands and a dipyridylamine motif as N^N ligand [13,14]. They proved to be efficient catalysts under photoredox conditions in a model aza-Henry reaction [13]. Herein, we wish to report the inhibition properties of TNF-α with 51 iridium(III) heteroleptic organometallic complexes.

2. Material and methods

2.1. General procedure GP1 for the synthesis of [Ir(C^N)$_2$(N^N)][PF$_6$] complexes

In a dry flamed Schlenk tube under argon atmosphere, iridium dimers (1 eq.) and N^N ligands (2.2 eq.) were introduced in degassed 2:1 mixture of dichloromethane/methanol (8 mL). The reaction mixture was stirred at 50 °C for 6 h. After cooling down the solution to room temperature, excess of KPF$_6$ (10 eq.) was added affording a precipitate. The inorganic solid was filtered off and the filtrate was evaporated. The solid was washed on a frit with diethyl ether (3 × 5 mL) and dried under vacuum to afford pure cationic iridium [Ir(C^N)$_2$(N^N)][PF$_6$] complexes.

2.2. General procedure GP2 for the synthesis of neutral [Ir(C^N)$_2$(acac)] complexes

In a flamed-dried Schlenk tube under argon atmosphere, iridium dimers (1 eq.) and acac ligands (5 eq.) were introduced in a degassed solution of ethoxyethanol with K$_2$CO$_3$ (10 eq.). The reaction mixture was stirred at 100 °C for 24 h. After cooling down the solution to room temperature, water was added affording a precipitate. The resulting precipitate was collected on a frit and washed with water (5 mL) and diethyl ether (5 mL) and finally dried under vacuum to afford pure complexes.

2.3. TNF-α–TNFR-1 binding ELISA procedure

This assay was carried following a known protocol [10]. Briefly, microtiter plates were coated overnight with TNF-α (0.625 μg/mL) in 100 μL PBS at 4 °C. The wells were washed three times with 200 μL PBS/0.05% Tween 20 (PBST), blocked with 200 μL PBST containing 1% BSA for 60 min and washed as before. Dilutions of the test compounds (100 μM) in 50 μL PBS containing 2% DMSO were added to the wells and the microtiter plates were incubated with shaking for 20 min. TNFR-1 (0.2 μg/mL) in 50 μL PBS was added to the wells and the plates were incubated for a further 120 min. The plates were washed as before and incubated for 120 min with TNFR-1 antibody (1:1000) in 100 μL PBST containing 1% BSA. The plates were washed three times with PBST and incubated for 90 min with anti-rabbit cross adsorbed-peroxidase secondary antibody (8 μg/mL) in 100 μL PBS. The plates were washed as before and incubated with 100 μL TMB solution, quenched with 100 μL 2 N chlorhydric acid and the absorbance was measured at λ = 450 nm.

2.4. Influence of light on ELISA procedure

Microtiter plates were coated overnight with TNF-α (0.625 μg/mL) in 100 μL PBS at 4 °C. The wells were washed three times with 200 μL PBS/0.05% Tween 20 (PBST), blocked with 200 μL PBST containing 1% BSA for 60 min and washed as before. Test compounds (100 μM) in 50 μL PBS containing 2% DMSO were added to the wells and the microtitre plates were incubated with shaking for 20 min, under blue LED strip (FlexLed inspire®, 2.4 W/m) or obscurity. TNFR-1 (0.2 μg/mL) in 50 μL PBS was added to the wells and the plates were incubated for a further 120 min under blue LED strip or obscurity. The plates were washed as before and incubated for 120 min under blue LED strip or obscurity with TNFR-1 antibody (1:1000) in 100 μL PBST containing 1% BSA. The plates were washed three times with PBST and incubated for 90 min under blue LED strip or obscurity with anti-rabbit cross adsorbed-peroxidase

secondary antibody (8 μg/mL) in 100 μL PBS. The plates were washed as before and incubated with 100 μL TMB solution, quenched with 100 μL 2 N chlorhydric acid and the absorbance was measured at λ = 450 nm.

2.5. Synergic tests procedure

Microtiter plates were coated overnight with TNF-α (0.625 μg/mL) in 100 μL PBS at 4 °C. The wells were washed three times with 200 μL PBS/0.05% Tween 20 (PBST), blocked with 200 μL PBST containing 1% BSA for 60 min and washed as before. Two of the test compounds (100 μM) in 25 μL PBS containing 2% DMSO were combined and added to the wells, following the same procedure, **4a**, **1c**, **3c** (100 μM) in 16.66 μL PBS containing 2% DMSO were combined and added to the wells. The microtiter plates were incubated with shaking for 20 min. TNFR-1 (0.2 μg/mL) in 50 μL PBS was added to the wells and the plates were incubated for a further 120 min. The plates were washed as before and incubated for 120 min with TNFR-1 antibody (1:1000) in 100 μL PBST containing 1% BSA. The plates were washed three times with PBST and incubated for 90 min with anti-rabbit cross adsorbed-peroxidase secondary antibody (8 μg/mL) in 100 μL PBS. The plates were washed as before and incubated with 100 μL TMB solution, quenched with 100 μL 2 N chlorhydric acid and the absorbance was measured at λ = 450 nm.

2.6. Blue native PAGE analysis of TNF-α–1c interaction

A solution of TNF-α (20 μM) in presence or absence of **1c** (100 μM) was analyzed using Blue-Native PAGE in 12% Polyacrylamide resolving gel following reported procedures [15].

3. Results and discussion

Only one iridium cationic complex has been previously described for TNF-α inhibition [10]. In this work, we prepared a series of 51 racemic iridium(III) complexes, both neutral and cationic, in order to give a good overview of the structure-function relationships (Table 1).

Such complexes can be easily obtained with high isolated yields ranging from 47 to 99%, *via* a two steps synthesis following known procedures (see Scheme 1 and E.S.I) [13,16]. Their structures were assessed by comparison with known X-ray structure of previously published iridium complexes and by NMR (see E.S.I.). Amongst them, 21 were never previously chemically synthesized and characterized (in italics in the table). In our study, we thus decided to select four cyclometalated C^N ligands 2-phenylpyridine (ppy) **a**, 1-phenylpyrazole (ppz) **b**, 7,8-benzoquinoline (bzq) **c** and 1-phenylisoquinoline (piq) **d** and eleven ancillary N^N ligands 2,2′-bipyridine (bpy) **1** and its dimethyl analogue (4-Me-bpy) **2**, 1,10-phenanthroline (phen) **3**, 2,9-dimethyl-1,10-phenanthroline (neo) **4**, 3,4,7,8-tetramethyl-1,10-phenanthroline (tphen) **5**, 2,2′-dipyridylmethane (dpm) **6**, 2,2′-dipyridylamine (dpa) **7** and its 3-, 4- and 5-dimethyl analogues, (3-Me-dpa) **8**, (4-Me-dpa) **9** and (5-Me-dpa) **10** respectively, or *N*-methyl derivative (*N*-Me-dpa) **11**. Combination of these C^N and N^N ligands led to a series of 42 cationic complexes (C^N = **a**-**d**, N^N = **1**–**11**, see Table 1). In addition, three anionic ligands namely the anion of dpa (dpa^-) **12**, the anion of the dibenzoylmethanate (dbm) **13** and the acetylacetonate (acac) **14** allowed us to obtain 9 neutral complexes (C^N = **a**-**d**, N^N = **12**, O^O = **13**–**14**, see Table 1).

With these complexes in hands, we investigated their capacity in inhibiting the TNF-α/TNF Receptor-1 interaction, using an ELISA experiment to determine the half-maximal inhibitory concentration (IC_{50}) values. Similar conditions than previously reported were used to facilitate the comparison [10]. Briefly microtiter plates coated with TNF-α were incubated with TNFR-1 together with racemic complexes. TNFR-1 binding was detected using anti-TNFR-1 antibody and horseradish peroxidase-conjugated secondary antibody, by measuring the absorbance at 450 nm.

Unsurprisingly, all the complexes demonstrated to be inhibitors, going from really poor to highly potent ones (Table 2). Amongst them, 10 complexes were able to inhibit the interaction at more than 50% at a concentration of 50 μM, three complexes were even more potent and only let less than 40% residual binding. Indeed, like protein-protein interactions were mostly occurring through hydrophobic interactions, and as reported by Leung et al. [10], aromatic ligands were expected to be able to interact with the β-strands of the binding site of the dimeric form of TNF-α. Such results suggested that the size of the complex and the nature of the ancillary ligands are of utmost importance for the TNF-α inhibitory activity. More precisely, series **a** and **c** demonstrated to be more potent than **b** and **d**, with average residual binding values of 56.2% and 47.2% against 61.7% and 71.0% respectively. Lower inhibitory activities were observed with the piq ligands compared to the ppy ones. Such result might be explained by the steric hindrance of the isoquinoline moiety. Therefore, in our study, the best C^N ligand was bzq, slightly better than ppy ligand previously reported by Leung et al. [10] N^N ligands were also crucial for the interactions and small changes could have terrible impact. For example, the addition of methyl substituents could greatly increase the biological properties, as shown by going from complex **3a** to **4a** or **5a**. In an overall manner, polyaromatic substituents are more effective (phen > bpy and dpa). This trend might be also correlated with the planarity of the N^N ligands. A negative charge on the N^N ligand appeared to be unfavourable (dpa compared to dpa^-). It is noteworthy that acac ligands displayed interesting biological properties, despite giving neutral iridium(III) complexes. As a consequence, the three best complexes were **1c**, **3c** and **4a**, with IC_{50} values of 25 ± 16 μM, 34 ± 3 μM and 48 ± 7 μM, respectively.

In a second series of experiments, a 1/1 mixture of two different complexes **4a**, **1c** or **3c** was used in the ELISA tests. Surprisingly, all reactions demonstrated an increased inhibitory activity going from 9% to 19%, but yet unexplained (Fig. 2). The best synergic effect was observed when the two complexes **3c** and **4a** where mixed. A 1/1/1 mixture of the three complexes proved also to be more efficient that one complex alone, but to a lesser extent than the latter one. Interestingly, this effect cannot simply be attributed to ligand exchange since none were observed as demonstrated by NMR correlation studies of the different mixtures (see E.S.I.).

Finally, the influence of the nature of the light was evaluated in ELISA tests with our three best complexes **1c**, **3c** and **4a** (Fig. 3 up). In the absence of light, the complexes were less potent. Interestingly, the blue light induced an increase in the inhibitory activity from 6% to 15%, and the white light was the most effective with an increase up to 21%. In fact, all theses three complexes, including either a ppy and/or bzq ligand, have previously demonstrated to present a maximum of absorption which can be ascribed to a π–π* ligand-centred (LC) transition, in the UV region as well as a weak and broad band of absorption at 425 nm, that corresponds to a dπ-π* metal-to-ligand charge transfer ([1]MLCT) (Fig. 3 bottom) [13]. They also proved to own photoredox capacities that might be at the origin of such increase activities. Such hypothesis was strengthened by the observed lower inhibitory activities with ppz-complexes (series **b**), which do not present any maximum of absorption in the visible region. Therefore the iridium complex might interact with the protein (and some amino acids) *via* a radical process and then might be not the same at the end of the irradiation period. However no change was observed using mass spectrometry of the protein in the presence of such complex nor of the iridium complex

Table 1
Series of Iridium (III) complexes C^N = **a**–**d**.

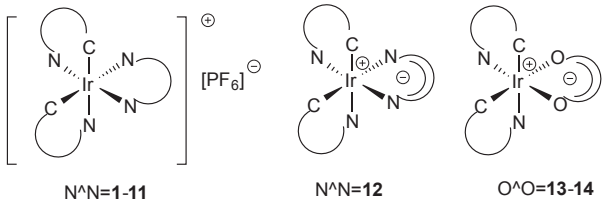

	C^N	**a** (ppy)	**b** (ppz)	**c** (bzq)	**d** (piq)
N^N		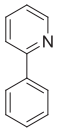	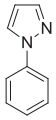	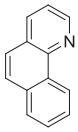	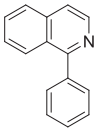
bpy **1**	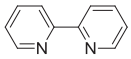	**1a**	**1b**	***1c***	**1d**
4-Me-bpy **2**	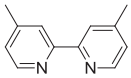	**2a**	***2b***	***2c***	**2d**
phen **3**	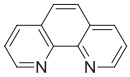	**3a**	**3b**	***3c***	**3d**
neo **4**	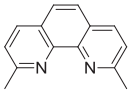	**4a**	***4b***	***4c***	***4d***
tphen **5**	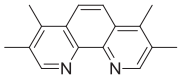	***5a***	***5b***	***5c***	***5d***
dpm **6**	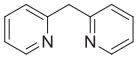	***6a***	***6b***	***6c***	***6d***
dpa **7**	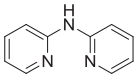	**7a**	**7b**	**7c**	**7d**
3-Me-dpa **8**	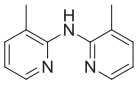	**8a**	**8b**	**8c**	**8d**
4-Me-dpa **9**	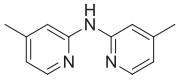	**9a**	**9b**	**9c**	**9d**
5-Me-dpa **10**	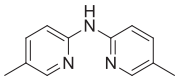	**10a**	**10b**	**10c**	**10d**
N-Me-dpa **11**	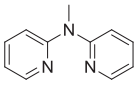	***11a***	–	–	***11d***
dpa^{-} **12**	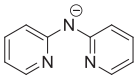	**12a**	**12b**	–	**12d**
O^O					
dbm **13**	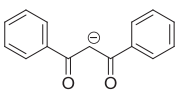	***13a***	***13b***	***13c***	–
acac **14**		**14a**	***14b***	**14c**	–

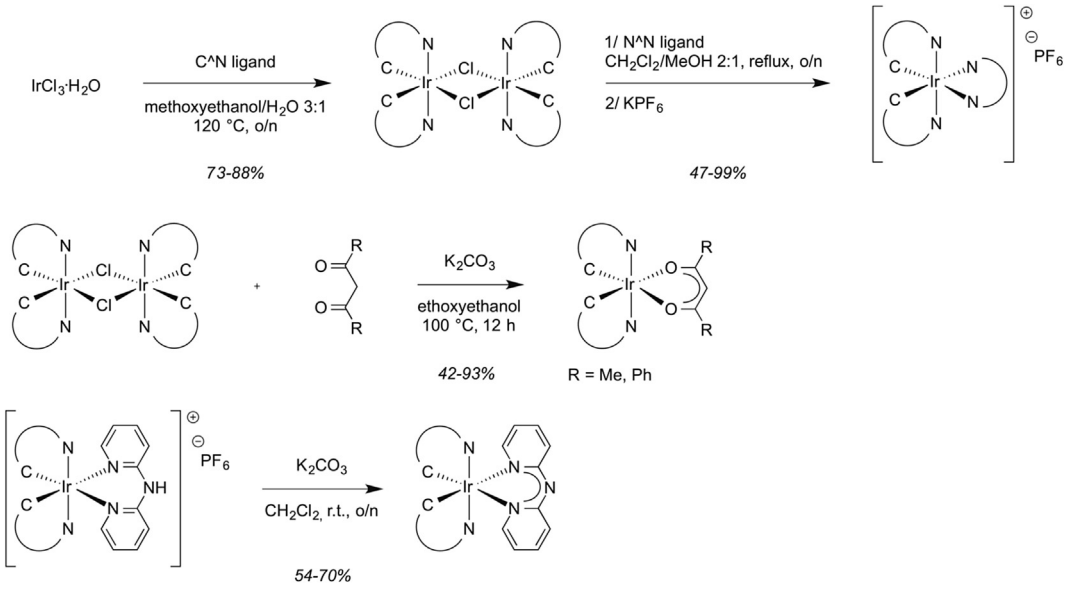

Scheme 1. Synthesis of the iridium complexes.

Table 2
Residual binding between TNF-α/TNF Receptor-1 when incubated with 50 μM of racemic iridium(III) complexes (each value represents the average of three individual measurements).

	a (ppy)	**b** (ppz)	**c** (bzq)	**d** (piq)
bpy **1**	62 ± 3	56 ± 6	44 ± 2	61 ± 3
4-Me-bpy **2**	63 ± 2	84 ± 4	59 ± 5	65 ± 7
phen **3**	95 ± 7	56 ± 5	36 ± 3	58 ± 5
neo **4**	37 ± 3	46 ± 5	56 ± 2	55 ± 7
tphen **5**	40 ± 3	80 ± 3	90 ± 2	73 ± 4
dpm **6**	48 ± 1	65 ± 1	57 ± 4	58 ± 1
dpa **7**	48 ± 3	66 ± 5	53 ± 3	55 ± 7
3-Me-dpa **8**	59 ± 4	58 ± 3	52 ± 2	73 ± 2
4-Me-dpa **9**	68 ± 3	91 ± 9	57 ± 1	78 ± 7
5-Me-dpa **10**	56 ± 2	63 ± 2	54 ± 4	69 ± 3
N-Me-dpa **11**	100	–	–	72 ± 1
dpa⁻ **12**	51 ± 2	78 ± 1	–	70 ± 8
dbm **13**	64 ± 7	55 ± 2	65 ± 2	–
acac **14**	46 ± 3	45 ± 2	44 ± 2	–

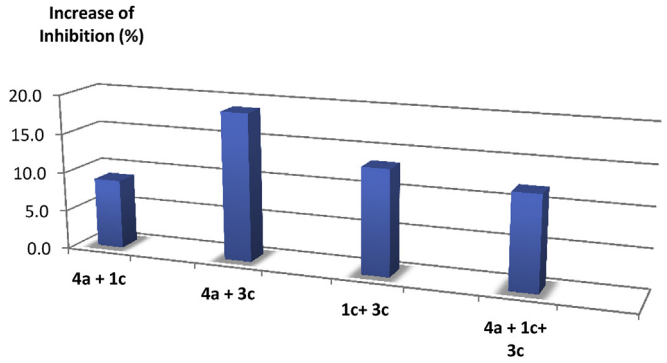

Fig. 2. Increase of inhibitory activity when incubated with 50 μM of equimolar mixture of multiple different racemic iridium(III) complexes.

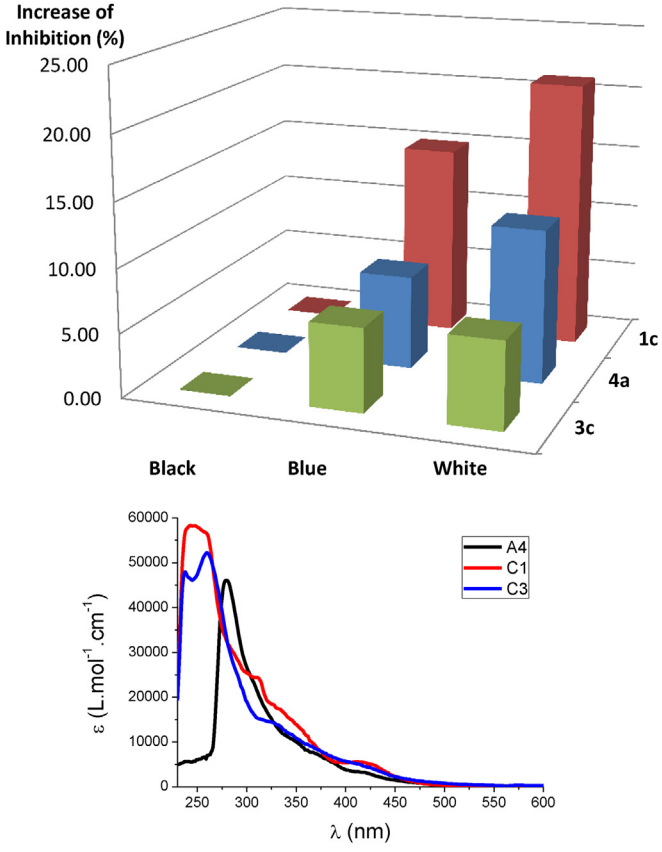

Fig. 3. (up) Increase of inhibitory activity when incubated with 50 μM of racemic iridium(III) complexes with different lights. (bottom) Absorption spectra of **1c**, **3c** and **4a**.

itself (data not shown). Another hypothesis is that, under visible light, the iridium is excited, and its geometry might be changed allowing better interactions with the protein.

The biologically active form of TNF-α corresponds to the trimer.

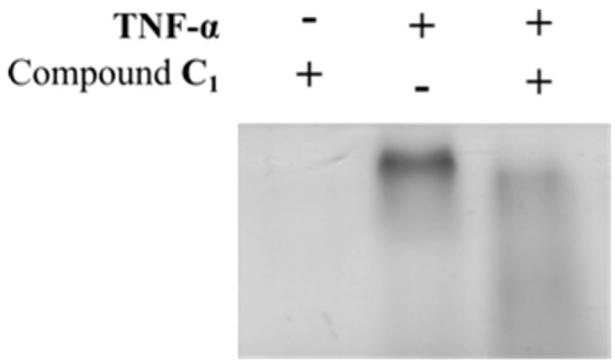

Fig. 4. Native Gel of TNF-α in the presence/absence of the racemic complex **1c**.

Indeed, previous works reported that small inhibitors like SPD304 were able to maintain the protein under its dimeric state, by promoting subunit dissociation [4]. Leung et al. postulated a similar biological mechanism when using the $[Ir(ppy)_2(biq)][PF_6]$ complex and used molecular modelling to assess their findings. However, in this latter case, no direct evidence of such interaction has been demonstrated so far. Through native gel analysis (Fig. 4), we were able to show that in the absence of **1c**, only one band corresponding to the trimeric form is present. However, in the presence of **1c**, this band disappeared to the profit of a very faint smear band, at a size corresponding to the dimeric form. This constitutes direct evidence and strongly supports the previous observation of Leung et al. [10].

4. Conclusions

In summary, we have easily and efficiently prepared 51 racemic iridium(III) complexes, both cationic and neutral. All of them have demonstrated their capacity to inhibit the TNF-α/TNF Receptor-1 interaction at various degrees. Structure-activity relationship studies emphasize the role of the size and the shape of the ancillary ligands for the binding. Interesting synergic effects were observed when using mixture of complexes. Moreover the nature of the light proved to be of utmost importance for the inhibitory activities. Our study gives a direct evidence of the binding of racemic iridium(III) complexes on the dimeric form of TNF-α. All together, these results pave the way for the development of efficient metal-based inhibitors that might have photo-diagnostic or -therapeutic applications. These studies are now ongoing in our laboratories.

Author contributions

The manuscript was written through contributions of all authors. All authors have given approval to the final version of the manuscript.

Acknowledgements

This work was supported by the “Ministère de la Recherche et des Nouvelles Technologies”, CNRS (Centre National de la Recherche Scientifique). The LABEX SynOrg (ANR-11-LABX-0029) is acknowledged for a PhD grant (E.S.). The authors thank the “Agence Nationale de la Recherche”, within the CSOSG program (ANR-12-SECU-0002-02), and the “Région Basse-Normandie” for funding (Post doc grant for R.M.).

Table of abbreviation

acac	acetylacetonate
bpy	2,2′-bipyridine
bzq	7,8-benzoquinoline
dpa	2,2′-dipyridylamine
dpm	2,2′-dipyridylmethane
LC	Ligand-Centred
MLCT	Metal-to-Ligand Charge Transfer
neo	2,9-dimethyl-1,10-phenanthroline
phen	1,10-phenanthroline
piq	1-phenylisoquinoline
ppy	2-phenylpyridine
ppz	1-phenylpyrazole
tphen	3,4,7,8-tetramethyl-1,10-phenanthroline
TNF	Tumor Necrosis Factor

Appendix A. Supplementary data

Supplementary data related to this article can be found at http://dx.doi.org/10.1016/j.jorganchem.2016.02.001.

References

[1] a) B. Rosenberg, L. VanCamp, J.E. Trosko, V.H. Mansour, Nature 222 (1969) 385–386; b) G. Gasser, I. Ott, N. Metzler-Nolte, J. Med. Chem. 54 (2011) 3–25.
[2] For recent reviews, see: a) I. Romero-Canelón, P.J. Sadler, Inorg. Chem. 52 (2013) 12276–12291; b) P.F. Salas, C. Herrmann, C. Orvig, Chem. Rev. 113 (2013) 3450–3492; c) N. Cutillas, G.S. Yellol, C. de Haro, C. Vicente, V. Rodríguez, J. Ruiz, Coord. Chem. Rev. 257 (2013) 2784–2797; d) A.K. Singh, D.S. Pandey, Q. Xu, P. Braunstein, Coord. Chem. Rev. 270–271 (2014) 31–56; e) B. Bertrand, A. Casini, Dalton Trans. 43 (2014) 4209–4219; f) A.A. Nazarov, C.G. Hartinger, P.J. Dyson, J. Organomet. Chem. 751 (2014) 251–260; g) F. Cisnetti, A. Gautier, Angew. Chem. Int. Ed. 52 (2013) 11976–11978; h) C.-H. Leung, S. Lin, H.-J. Zhong, D.-L. Ma, Chem. Sci. 6 (2015) 871–884; i) N.P.E. Barry, P.J. Sadler, Chem. Commun. 49 (2013) 5106–5131; j) C. Santini, M. Pellei, V. Gandin, M. Porchia, F. Tisato, C. Marzano, Chem. Rev. 114 (2014) 815–862; k) G. Süss-Fink, J. Organomet. Chem. 751 (2014) 2–19; l) Z. Liu, P.J. Sadler, Acc. Chem. Res. 47 (2014) 1174–1185; m) K.J. Kilpin, P.J. Dyson, Chem. Sci. 4 (2013) 1410–1419.
[3] B.B. Aggarwal, S.C. Gupta, J.H. Kim, Blood 119 (2012) 651–665.
[4] M.M. He, A.S. Smith, J.D. Oslob, W.M. Flanagan, A.C. Braisted, A. Whitty, M.T. Cancilla, J. Wang, A.A. Lugovskoy, J.C. Yoburn, A.D. Fung, G. Farrington, J.K. Eldredge, E.S. Day, L.A. Cruz, T.G. Cachero, S.K. Miller, J.E. Friedman, I.C. Choong, B.C. Cunningham, Science 310 (2005) 1022–1025.
[5] F. Giordanetto, A. Schafer, C. Ottmann, Drug Discov. Today 19 (2014) 1812–1821.
[6] H. Saito, T. Kojima, M. Takahashi, W.C. Horne, R. Baron, T. Amagasa, K. Ohya, K. Aoki, Arthritis Rheum. 56 (2007) 1164–1174.
[7] D.S.-H. Chan, H.-M. Lee, F. Yang, C.-M. Che, C.C.L. Wong, R. Abagyan, C.-H. Leung, D.-L. Ma, Angew. Chem. Int. Ed. 49 (2010) 2860–2864.
[8] Q. Shen, J. Chen, Q. Wang, X. Deng, Y. Liu, L. Lai, Eur. J. Med. Chem. 85 (2014) 119–126.
[9] a) D.-L. Ma, D.S.-H. Chan, C.-H. Leung, Acc. Chem. Res. 47 (2014) 3614–3631; b) C.-H. Leung, L. Liu, L. Lu, B. He, D.W.J. Kwong, C.-Y. Wong, D. Ma, Chem. Commun. 51 (2015) 3973–3976; c) C.-H. Leung, H. Zhong, D.S.H. Chan, D. Ma, Coord. Chem. Rev. 257 (2013) 1764–1776.
[10] C.-H. Leung, H.-J. Zhong, H. Yang, Z. Cheng, D.S.-H. Chan, V.P.-Y. Ma, R. Abagyan, C.-Y. Wong, D.-L. Ma, Angew. Chem. Int. Ed. 51 (2012) 9010–9014.
[11] S. Gaillard, M.K. Elmkaddem, C. Fischmeister, C.M. Thomas, J.-L. Renaud, Tetrahedron Lett. 49 (2008) 3471–3474.
[12] a) Z. Zheng, M.K. Elmkaddem, C. Fischmeister, T. Roisnel, C.M. Thomas, J.-F. Carpentier, J.-L. Renaud, New J. Chem. 32 (2008) 2150–2158; b) C. Romain, S. Gaillard, M.K. Elmkaddem, L. Toupet, C. Fischmeister, C.M. Thomas, J.-L. Renaud, Organometallics 29 (2010) 1992–1995.
[13] E. Sauvageot, R. Marion, F. Sguerra, A. Grimault, R. Daniellou, M. Hamel, S. Gaillard, J.-L. Renaud, Org. Chem. Front. 1 (2014) 639–644.
[14] F. Sguerra, R. Marion, G.H.V. Bertrand, R. Coulon, E. Sauvageot, R. Daniellou, J.L. Renaud, S. Gaillard, M. Hamel, J. Mater. Chem. C 2 (2014) 6125–6133.
[15] a) I. Wittig, H.-P. Braun, H. Schagger, Nat. Protoc. 1 (2006) 16–22; b) P. Ameloot, W. Declercq, W. Fiers, P. Vandenabeele, P. Brouckaert, J. Biol. Chem. 276 (2001) 27098–27103.
[16] M. Nonoyama, Bull. Chem. Soc. Jpn. 47 (1974) 767–768.